Supplementary information for

Crystal structure, phase transition and properties of indium(III) sulfide

Paweł Wyżga[a,b], Wilder Carrillo-Cabrera[b], Lev Akselrud[b,c], Igor Veremchuk[b,d], Jörg Wagler[e], Christoph Hennig[f,g], Alexander A. Tsirlin[h], Andreas Leithe-Jasper[b], Edwin Kroke[e], Roman Gumeniuk[a,*]

[a] Institut für Experimentelle Physik, TU Bergakademie Freiberg, Leipziger Straße 23, 09599 Freiberg, Germany

[b] Max-Planck-Institut für Chemische Physik fester Stoffe, Nöthnitzer Straße 40, 01187 Dresden, Germany

[c] Ivan Franko National University of Lviv, Kyryla and Mefodiya Str. 6, UA-79005, Lviv, Ukraine

[d] Institute for Ion Beam Physics and Materials Research, Helmholtz-Zentrum Dresden-Rossendorf, Bautzner Landstraße 400, 01328 Dresden, Germany

[e] Institut für Anorganische Chemie, TU Bergakademie Freiberg, Leipziger Straße 29, 09599 Freiberg, Germany

[f] Institute of Resource Ecology, Helmholtz-Zentrum Dresden-Rossendorf, Bautzner Landstraße 400, 01328 Dresden, Germany

[g] The Rossendorf Beamline BM20, European Synchrotron Radiation Facility, 71, avenue des Martyrs, 38043 Grenoble, France

[h] Experimental Physics VI, Center for Electronic Correlations and Magnetism, Institute of Physics, University of Augsburg, 86135 Augsburg, Germany

Table S1. Synthesis and heat treatment conditions for all studied samples together with unit cell parameters, experimental density (determined by immersion technique) and WDXS chemical compositions.

No.	Series [a]	Mass [g], Form	Heat treatment			Unit-cell parameters [b]				Density	WDXS
			Heating T [K] / t [h]	Annealing T [K] / t [h]	Cooling T [K] / t [h]	a [Å]	c [Å]	c/a	V [Å^3]	d [g·cm^{-1}]	composition [e]
1	B1	~ 2, In + S, powders	723/24	723/96	308/12	7.61914(5)	32.3238(4)	4.24245(6)	1876.44(3)		
2	B2	~ 1, from B1, pieces	873/24	873/168	Q_W	7.6197(2)	32.324(1)	4.2422(2)	1876.73(9)		
3	B3	~ 1, from B2, pieces	873/6	873/136	Q_N	7.6198(1)	32.3224(9)	4.2419(1)	1876.68(6)		
4	B4	~ 0.1, from B1, pieces	873/0.17	873/168	Q_W	7.61955(9)	32.3231(7)	4.2421(1)	1876.60(5)		
5	B6 [c]	0.015, from B3, powder	873/60	873/90	Q_N	7.61901(9)	32.3261(6)	4.24282(9)	1876.51(3)		
6	B7	0.138, from B1	1073/8	1073/80 (in liquid)	Q_N	7.6197(2)	32.328(1)	4.2427(2)	1876.96(9)		
7	SPS (B3)	0.81, from B3	923/0.22	923/0.17	900/0.5	7.6193(1)	32.3253(9)	4.2426(1)	1876.60(6)	4.568(6)	$In_{2.66(1)}S_{4.00(1)}$
8	LFA (B3)	round pellet	773/~12	-	773/~12	7.6199(1)	32.3245(9)	4.2421(1)	1876.85(9)		
9	ZEM (B3)	rectangular bar	773/~8	-	773/~8	7.6192(2)	32.323(1)	4.2423(2)	1876.42(9)		
10	C1 [d]	~ 2, In + S (excess)	873/24	873/168	Q_W	7.61893(9)	32.3248(6)	4.24270(9)	1876.39(5)		
11	SPS (C1#1)	~ 0.85, from C1	923/0.22	923/0.17	900/0.5	7.61920(7)	32.3251(5)	4.24258(8)	1876.54(4)	4.584(6)	
12	LFA (C1#2)	round pellet	773/~12	-	773/~12	7.6202(2)	32.323(2)	4.2418(3)	1876.9(1)	4.580(8)	
13	SC1	~ 0.9, $In_{2.67}S_4$ + S + I	1123/362	1123→1073/312	air quenching + Q_W	7.61911(4)	32.3281(3)	4.24303(5)	1876.67(2)		$In_{2.67(1)}S_{4.00(1)}$
						Pseudo-cubic value: c/a = 3√2 =		4.24264			

[a] B1-B6 samples were reported in our previous work[10] and we kept the same labels for unification. [b] Presented unit-cell parameters were determined using LaB_6 as internal standard. [c] B6 sample was manually ground and sealed in a quartz capillary ϕ = 0.5 mm before annealing. [d] C1 sample was additionally annealed in S-vapor at 873 K for 1h. [e] As a standard material, we used the SC1 sample annealed in sulfur vapor. SC1 - single crystal. Q_W/Q_N - quenching in iced water/liquid nitrogen.

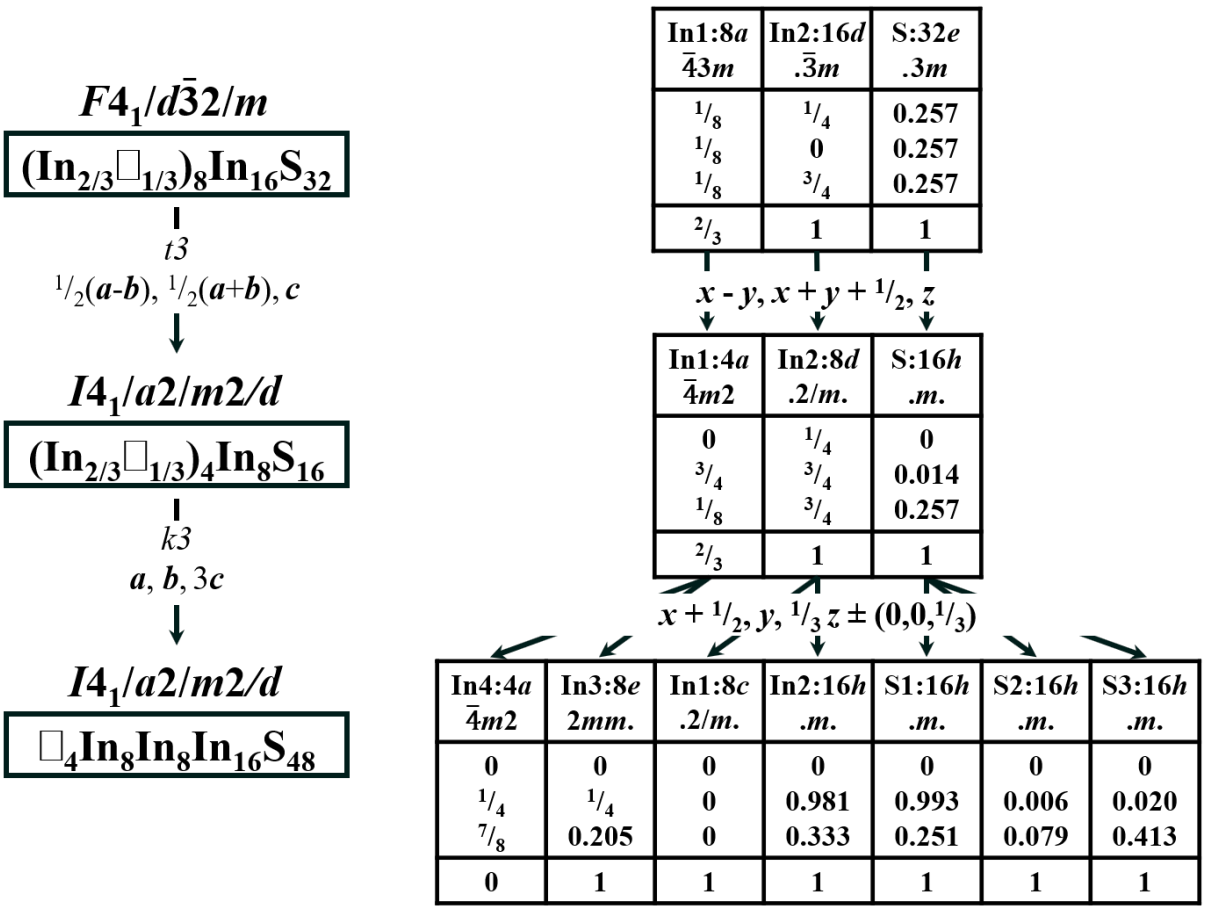

Figure S1.Group-subgroup relation in the form of a Bärnighausen scheme (atom type, Wyckoff position, site symmetry, atomic coordinates and site occupancy factor) for the cubic (873 K) and the tetragonal (80 K) modification of $In_{0.67}\square_{0.33}In_2S_4$. Coordinates for both space groups are presented according to Origin Choice 2. The intermediate structure is not observed for $In_{0.67}\square_{0.33}In_2S_4$.

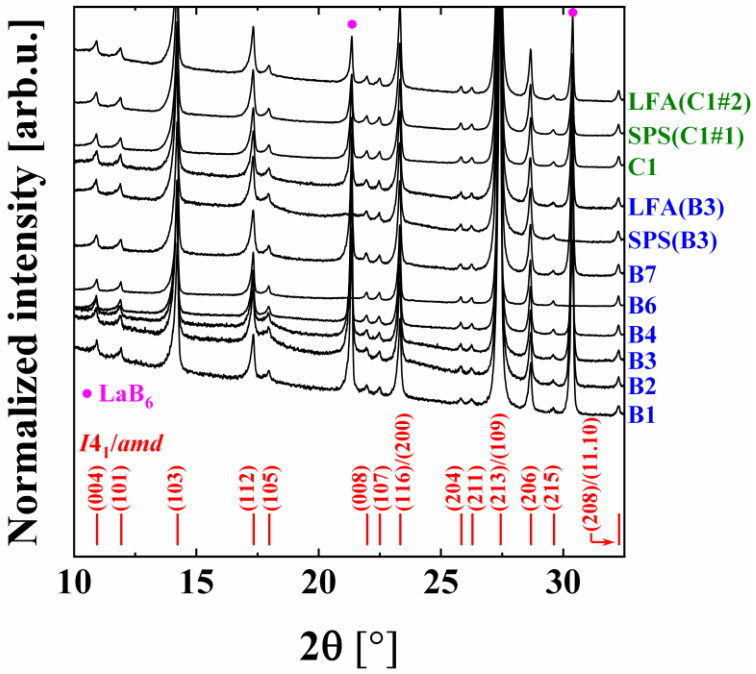

Figure S2. Laboratory PXRD patterns for the studied polycrystalline samples. LaB_6 was used as an internal standard for unit-cell parameter refinements.

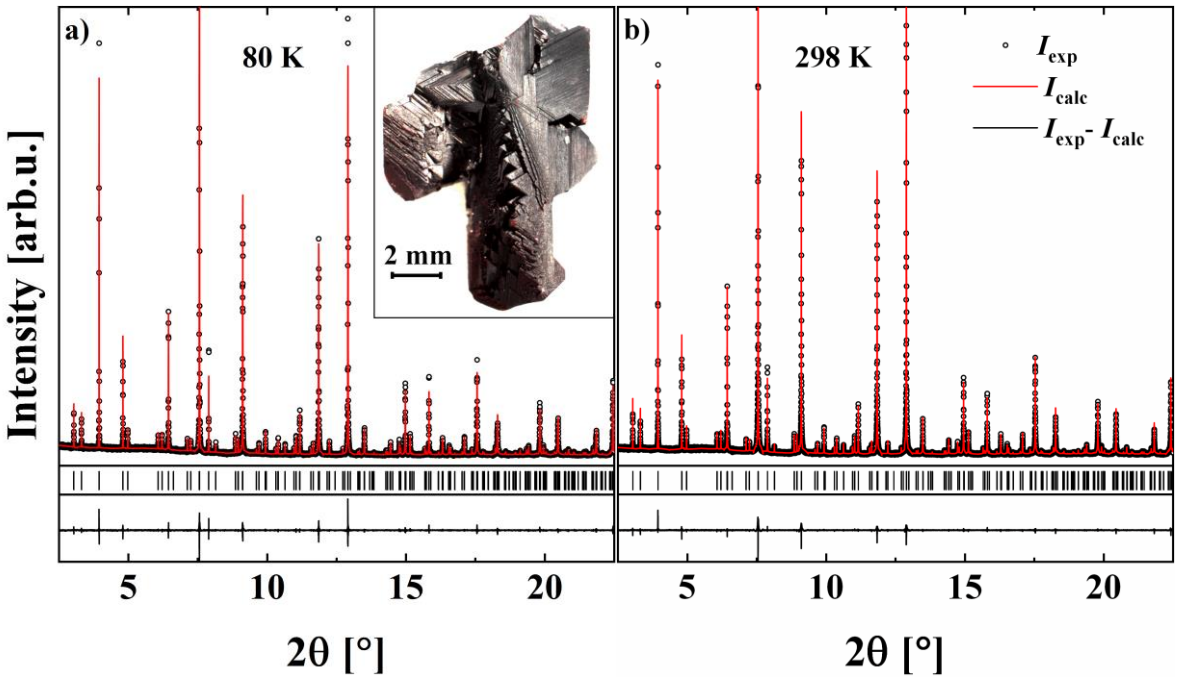

Figure S3. Rietveld refinement of the powdered SC1 sample. Diffraction data were taken at 80 (a) and 298 K (b) with λ = 0.42768 Å. Inset in a): as-grown aggregate of β-$In_{0.67}\square_{0.33}In_2S_4$ crystals used for the structural studies.

Table S2. Crystallographic data for the β-$In_{0.67}\square_{0.33}In_2S_4$ (powdered SC1-sample) at 80 and 293 K obtained from Rietveld refinements.

Temperature [K]	**80**	**298**
Chemical composition	In_2S_3	
Space group, Pearson symbol	$I4_1/amd$ (no. 144), $tI80$	
a [Å]	7.60670(4)	7.62091(8)
c [Å]	32.3008(2)	32.3401(7)
V [Å^3]	1868.99(3)	1878.26(8)
d [g·cm^{-3}]	4.6313(1)	4.6089(2)
λ [Å]	0.42768	
$2\theta_{max}$ [°], sinθ/λ (max)	42.13, 0.84	40, 0.80
No. of refined reflections	1243	1136
R_I, R_P [%]	3.13, 15.98	5.15, 15.65
In1 at 8c (0 0 0) / U_{iso} [Å^2]	0.012(2)	0.025(3)
In2 at 16h (0 y z) / U_{iso} [Å^2]	0.9811(3), 0.3325(2) / 0.013(1)	0.9815(6), 0.3328(3) / 0.021(2)
In3 at 8e (0 $^1/_4$ z) / U_{iso} [Å^2]	0.2050(2) / 0.011(1)	0.2052(3) / 0.019(1)
S1 at 16h (0 y z) / U_{iso} [Å^2]	0.993(1), 0.2512(3) / 0.013(5)	0.988(3), 0.251(1) / 0.014(7)
S2 at 16h (0 y z) / U_{iso} [Å^2]	0.006(1), 0.0790(4) / 0.012(4)	0.008(3), 0.079(1) / 0.021(7)
S3 at 16h (0 y z) / U_{iso} [Å^2]	0.020(1), 0.4130(4) / 0.010(4)	0.024(3), 0.414(1) / 0.013(6)
4 × In1-S1, 2 × In1-S2 [Å]	2.653(7), 2.55(1)	2.62(2), 2.57(3)
1 × In2-S1, 2 × In2-S2, 1 × In2-S3, 2 × In2-S3 [Å]	2.63(1), 2.561(7), 2.61(2), 2.694(6)	2.66(3), 2.55(2), 2.65(3), 2.67(2)
2 × In3-S1, 2 × In3-S3 [Å]	2.46(1), 2.46(1)	2.48(3), 2.49(3)

Table S3. Anisotropic displacement parameters U^{ij} [Å^2] from single-crystal refinement of β-$In_{0.67}\square_{0.33}In_2S_4$ (sample SC1). The anisotropic-displacement-factor exponent takes the form: $-2\pi^2[h^2 \cdot a^{*2} \cdot U^{11} + \ldots + 2h \cdot k \cdot a^* \cdot b^* \cdot U^{12}]$.

Atom	U^{11}	U^{22}	U^{33}	U^{23}	U^{13}	U^{12}
In1 (8c)	0.0207(8)	0.0120(8)	0.0179(9)	-0.0022(5)	0	0
In2 (16h)	0.0211(5)	0.0117(4)	0.0182(6)	-0.0030(4)	0	0
In3 (8e)	0.0153(5)	0.0169(6)	0.0122(6)	0	0	0
S1 (16h)	0.016(2)	0.015(2)	0.015(2)	-0.001(1)	0	0
S2 (16h)	0.017(2)	0.014(2)	0.016(2)	-0.000(1)	0	0
S3 (16h)	0.013(2)	0.011(1)	0.012(2)	0.000(1)	0	0

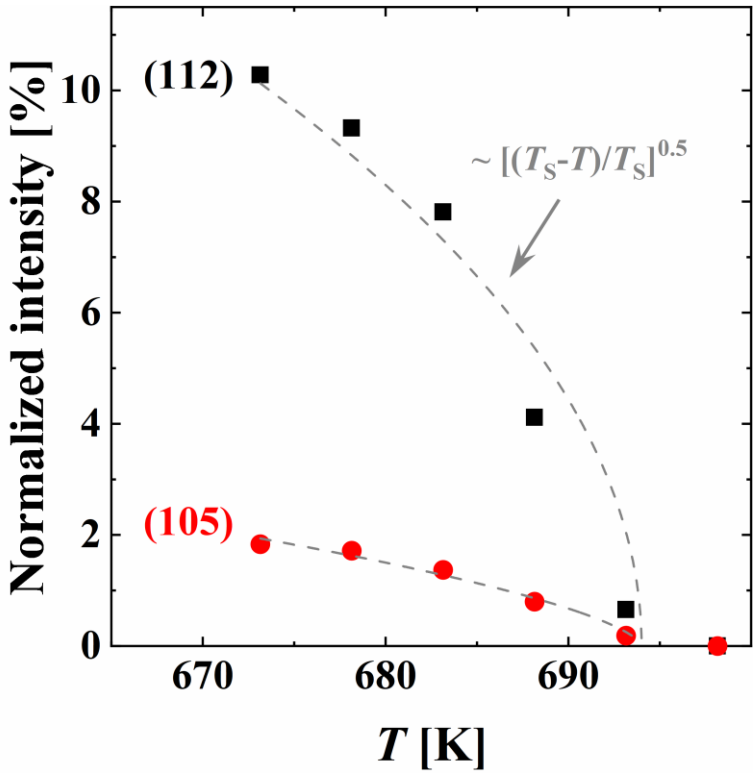

Figure S4. Temperature evolution of the intensity of satellite reflections (112) and (105) near the phase transition. Dashed lines indicate $I \sim \left[\frac{(T_S-T)}{T_S}\right]^{0.5}$ dependence with T_S = 694 K.

Table S4. Crystallographic data for the $In_{0.67}\square_{0.33}In_2S_4$ (sample B3) at 298–673 K obtained from Rietveld refinements with the tetragonal $I4_1/amd$ space group.

	Temperature [K]				
	298	**373**	**473**	**573**	**673**
Refined composition	In_2S_3				
Space group, Pearson symbol	$I4_1/amd$ (no. 144), $tI80$				
a [Å]	7.6210(3)	7.6271(3)	7.6351(2)	7.6438(2)	7.6525(2)
c [Å]	32.317(2)	32.339(2)	32.366(2)	32.395(2)	32.422(2)
V [Å^3]	1876.9(2)	1881.2(2)	1886.8(2)	1892.8(2)	1898.7(2)
d [g·cm^{-3}]	4.6121(5)	4.6016(6)	4.5881(5)	4.5736(5)	4.5593(5)
λ [Å]	0.73138				
$2\theta_{max}$ [°], $\sin\theta/\lambda$ (max)	34.98, 0.411				
No. of refined reflections	169	170	170	170	170
R_I, R_P [%]	2.22, 5.01	2.13, 5.31	2.23, 5.30	2.26, 5.43	2.29, 5.68
In1 at 8c (0 0 0) / U_{iso} [Å^2]	0.030(1)	0.032(1)	0.037(1)	0.043(2)	0.050(2)
In2 at 16h (0 y z) / U_{iso} [Å^2]	0.9813(3), 0.3327(1) / 0.0265(7)	0.9812(3), 0.3327(2) / 0.0320(8)	0.9812(3), 0.3327(2) / 0.0364(8)	0.9811(3), 0.3328(2) / 0.0415(9)	0.9822(3), 0.3329(2) / 0.0480(9)
In3 at 8e (0 $^1/_4$ z) / U_{iso} [Å^2]	0.2044(1) / 0.0239(7)	0.2044(1) / 0.0278(7)	0.2044(1) / 0.0312(7)	0.2046(2) / 0.0358(8)	0.2051(2) / 0.0422(8)
S1 at 16h (0 y z) / U_{iso} [Å^2]	0.996(2), 0.2522(5) / 0.013(3)	0.997(2), 0.2520(5) / 0.023(4)	0.996(2), 0.2515(5) / 0.025(4)	0.995(2), 0.2512(5) / 0.033(4)	0.993(2), 0.2509(5) / 0.041(5)
S2 at 16h (0 y z) / U_{iso} [Å^2]	0.006(2), 0.0768(5) / 0.029(4)	0.006(2), 0.0769(6) / 0.027(4)	0.007(2), 0.0771(5) / 0.032(4)	0.008(2), 0.0774(5) / 0.036(4)	0.008(1), 0.0777(5) / 0.046(4)
S3 at 16h (0 y z) / U_{iso} [Å^2]	0.018(2), 0.4130(6) / 0.026(3)	0.018(2), 0.4129(6) / 0.029(3)	0.018(2), 0.4134(6) / 0.032(3)	0.019(1), 0.4143(6) / 0.034(4)	0.020(1), 0.4150(5) / 0.035(4)

Table S5. Crystallographic data for the $In_{0.67}\square_{0.33}In_2S_4$ (sample B3) at 678–688 K obtained from Rietveld refinements with the tetragonal $I4_1/amd$ space group.

	Temperature [K]		
	678	**683**	**688**
Refined composition	In_2S_3		
Space group, Pearson symbol	$I4_1/amd$ (no. 144), $tI80$		
a [Å]	7.6531(2)	7.6537(3)	7.6547(6)
c [Å]	32.424(2)	32.426(2)	32.435(4)
V [Å^3]	1899.1(2)	1899.5(3)	1900.5(6)
d [g·cm^{-3}]	4.5583(5)	4.5573(6)	4.555(2)
λ [Å]	0.73138		
$2\theta_{max}$ [°], $\sin\theta/\lambda$ (max)	34.98, 0.411		
No. of refined reflections	170	170	170
R_I, R_P [%]	2.25, 5.92	2.33, 6.50	2.82, 9.11
In1 at 8c (0 0 0) / U_{iso} [Å^2]	0.050(2)	0.050(2)	0.049(3)
In2 at 16h (0 y z) / U_{iso} [Å^2]	0.9831(3), 0.3329(2) / 0.049(1)	0.9845(4), 0.3330(2) / 0.050(1)	0.9892(8), 0.3331(3) / 0.051(2)
In3 at 8e (0 $^1/_4$ z) / U_{iso} [Å^2]	0.2054(2) / 0.0440(9)	0.2058(2), 0.046(1)	0.2069(3) / 0.052(2)
S1 at 16h (0 y z) / U_{iso} [Å^2]	0.993(2), 0.2510(5) / 0.042(5)	0.991(2), 0.2509(5) / 0.045(6)	0.984(4), 0.251(1) / 0.05(1)
S2 at 16h (0 y z) / U_{iso} [Å^2]	0.007(1), 0.0778(5) / 0.049(5)	0.005(2), 0.0785(6) / 0.050(5)	0.999(3), 0.081(1) / 0.053(9)
S3 at 16h (0 y z) / U_{iso} [Å^2]	0.020(1), 0.4150(5) / 0.033(4)	0.020(2), 0.4149(6) / 0.029(4)	0.019(3), 0.415(1) / 0.022(7)

Standard deviations for isotropic displacement parameters and coordinates, and reliability factors R_I and R_P are significantly larger than in the refinements for temperatures lower than 678 K.

Table S6. Crystallographic data for the $In_{0.67}\square_{0.33}In_2S_4$ (sample B3) at 678–698 K obtained from Rietveld refinements with the tetragonal $I4_1/amd$ space group and partially occupied tetrahedral 4*a* and 8*e* sites.

	Temperature [K]			
	678	**683**	**688**	**693**
Refined composition	In_2S_3			
Space group, Pearson symbol	$I4_1/amd$ (no. 144), *tI*80			
a [Å]	7.6532(2)	7.6539(2)	7.6553(2)	7.6558(3)
c [Å]	32.423(2)	32.425(2)	32.431(2)	32.440(2)
V [Å^3]	1899.1(2)	1899.5(2)	1900.6(2)	1901.4(3)
d [g·cm^{-3}]	4.5583(5)	4.5573(5)	4.5548(5)	4.5528(6)
λ [Å]	0.73138			
$2\theta_{max}$ [°], $\sin\theta/\lambda$ (max)	34.98, 0.411			
No. of refined reflections	170			
R_I, R_P [%]	2.23, 5.53	2.20, 5.51	2.20, 5.36	2.22, 5.22
In1 at 8*c* (0 0 0) / U_{iso} [Å^2]	0.051(2)	0.051(2)	0.053(2)	0.051(4)
In2 at 16*h* (0 *y z*) / U_{iso} [Å^2]	0.9826(3), 0.3329(2) / 0.049(1)	0.9839(3), 0.3330(2) / 0.051(1)	0.9882(4), 0.3332(2) / 0.054(1)	0.9917(9), 0.3348(3) / 0.055(2)
In3 at 8*e* (0 $^1/_4$ *z*) / U_{iso} [Å^2]	0.2049(2) / 0.0420(8)	0.2051(2) / 0.0424(9)	0.2057(2) / 0.0441(9)	0.2076(4) / 0.047(3)
In4 at 4*a* (0 $^1/_4$ $^7/_8$) / U_{iso} [Å^2]	0.044$^+$	0.044$^+$	0.044$^+$	0.040(6)
S1 at 16*h* (0 *y z*) / U_{iso} [Å^2]	0.994(1), 0.2511(4) / 0.041(5)	0.993(1), 0.2511(4) / 0.042(5)	0.990(2), 0.2512(4) / 0.041(6)	0.983(3), 0.2516(8) / 0.043(7)
S2 at 16*h* (0 *y z*) / U_{iso} [Å^2]	0.008(1), 0.0776(5) / 0.045(4)	0.008(1), 0.0778(5) / 0.044(4)	0.009(1), 0.0784(5) / 0.046(5)	0.016(2), 0.0812(7) / 0.043(7)
S3 at 16*h* (0 *y z*) / U_{iso} [Å^2]	0.019(1), 0.4147(5) / 0.038(4)	0.019(1), 0.4148(5) / 0.038(4)	0.019(1), 0.4152(5) / 0.040(5)	0.006(3), 0.4129(7) / 0.041$^+$
Site occupancy factor of 8*e**	0.977(4)	0.955(4)	0.885(4)	0.684(8)
Site occupancy factor of 4*a**	0.047(6)	0.090(6)	0.229(7)	0.63(2)

$^+$ refinement yielded unreliably high U_{iso} value and thus the parameter was fixed. * Site occupancy factors (SOF) of 8*e* and 4*a* sites fulfill the constrain: SOF(8*e*) + $^1/_2$SOF(4*a*) = 1.

Table S7. Crystallographic data for the $In_{0.67}\square_{0.33}In_2S_4$ (sample B3) at 693 and 698 K obtained from two-phase Rietveld refinements with the tetragonal $I4_1/amd$ and cubic $Fd\bar{3}m$ phases.

	Temperature [K]		
	683	**688**	**693**
		Phase 1	
Assumed compositions	In_2S_3		
Space group, Pearson symbol	$I4_1/amd$ (no. 144), $tI80$		
a [Å]	7.6544	7.6547	7.6536
c [Å]	32.422	32.435	32.458
V [Å^3]	1899.6	1900.5	1901.3
d [g·cm^{-3}]	4.5572	4.5548	4.5530
λ [Å]	0.73138		
$2\theta_{max}$ [°], sinθ/λ (max)	34.98, 0.411		
No. of refined reflections	170		
R_I, R_P [%]	3.06, 6.16	4.19, 6.16	11.94, 6.49
In1 at 8c (0 0 0) / U_{iso} [Å^2]	0.050(3)	0.048(1)	0.047(5)
In2 at 16c (0 y z) / U_{iso} [Å^2]	0.9793(4), 0.3329(2) / 0.046(1)	0.9811(2), 0.3330(1) / 0.048(1)	0.994(1), 0.3332(5) / 0.049(3)
In3 at 8e (0 $^1/_4$ z) / U_{iso} [Å^2]	0.2037(2) / 0.041(1)	0.2041(1) / 0.037(1)	0.2075(6) / 0.058(4)
S1 at 16h (0 y z) / U_{iso} [Å^2]	0.997(2), 0.2512(6) / 0.033(7)	0.996(1), 0.2509(2) / 0.038(2)	0.978(4), 0.249(1) / 0.04(2)
S2 at 16h (0 y z) / U_{iso} [Å^2]	0.007(2), 0.0767(6) / 0.035(6)	0.005(1), 0.0765(2) / 0.038(2)	0.994(4), 0.084(1) / 0.05(2)
S3 at 16h (0 y z) / U_{iso} [Å^2]	0.017(2), 0.4144(7) / 0.040(6)	0.017(1), 0.4145(3) / 0.038(2)	0.024(4), 0.414(1) / 0.02(1)
Phase fraction [%]	63.6(9)	37.5(7)	14.1(2)
		Phase 2	
Assumed compositions	$In_{2.67}S_4$		
Space group, Pearson symbol	$Fd\bar{3}m$ (no. 227), $cF56(53.3)$		
a [Å]	10.8190	10.8212	10.8224
V [Å^3]	1266.4	1267.2	1267.6
d [g·cm^{-3}]	4.5612	4.5536	4.5522
λ [Å]	0.73138		
$2\theta_{max}$ [°], sinθ/λ (max)	34.98, 0.411		
No. of refined reflections	29		
R_I, R_P [%]	3.16, 6.16	2.23, 6.16	2.12, 6.49
In1 at 8a ($^1/_8$ $^1/_8$ $^1/_8$) / U_{iso} [Å^2]	0.0388(1)	0.049(1)	0.047(1)
In2 at 16d ($^1/_4$ 0 $^3/_4$) / U_{iso} [Å^2]	0.0568(1)	0.058(1)	0.055(1)
S at 32e (u u u) / U_{iso} [Å^2]	0.2573(1) / 0.050(1)	0.2569(3) / 0.046(2)	0.2572(2) / 0.040(1)
Phase fraction [%]	36.4(5)	62.5(6)	85.9(4)

Firstly, each pattern was refined assuming single-phase tetragonal or cubic structure. Then, a two-phase refinement was performed, starting from models obtained in the first step. The atomic coordinates and displacements parameters of the tetragonal polymorph and unit-cell parameters of both phases were fixed in the two-phase refinement due to a strong correlation between both structures.

Table S8. Crystallographic data for the $In_{0.67}\square_{0.33}In_2S_4$ (sample B3) at 703–873 K obtained from Rietveld refinements with the cubic $Fd\bar{3}m$ space group.

	Temperature [K]				
	698	**703**	**713**	**773**	**873**
Refined composition	$In_{2.67}S_4$				
Space group, Pearson symbol	$Fd\bar{3}m$ (no. 227), cF56(53.3)				
a [Å]	10.8234(2)	10.8239(2)	10.8249(2)	10.8311(2)	10.8421(2)
V [Å^3]	1267.91(6)	1268.08(6)	1268.43(6)	1270.64(7)	1274.49(8)
d [g·cm^{-3}]	4.5521(2)	4.5514(2)	4.5502(2)	4.5423(2)	4.5286(3)
λ [Å]	0.73138				
$2\theta_{max}$ [°], $\sin\theta/\lambda$ (max)	34.92, 0.410				
No. of refined reflections	29				
R_I, R_P [%]	1.25, 4.44	1.23, 4.49	1.23, 4.48	1.42, 4.72	2.08, 5.01
In1 at 8a ($^1/_8$ $^1/_8$ $^1/_8$) / U_{iso} [Å^2]	0.0459(9)	0.0460(9)	0.0460(9)	0.0505(9)	0.065(1)
In2 at 16d ($^1/_4$ 0 $^3/_4$) / U_{iso} [Å^2]	0.0558(6)	0.0558(6)	0.0557(6)	0.0587(6)	0.0625(8)
S at 32e (u u u) / U_{iso} [Å^2]	0.2571(2) / 0.042(1)	0.2571(2) / 0.042(1)	0.2570(2) / 0.042(1)	0.2569(2) / 0.043(1)	0.2569(2) / 0.045(1)
Site occupancy factor of 8a	0.667				

Table S9. Crystallographic data for the $In_{0.67}\square_{0.33}In_2S_4$ (sample B3) at 693 K obtained from Rietveld refinements with the modulated cubic $Fd\bar{3}m$(α,α,α)000(α,-α,-α)000(-α,α,-α)000 superspace group.

	Temperature [K]
	693
Refined composition	$In_{20.6}S_{32}$, 3392.77
Superspace group	*Fd-3m*(α,α,α)000(α,-α,-α)000(-α,α,-α)000
a [Å]	10.8228(6)
Wavevectors	$\begin{pmatrix} \boldsymbol{q}_1 \\ \boldsymbol{q}_2 \\ \boldsymbol{q}_3 \end{pmatrix} = \begin{pmatrix} \alpha & \alpha & \alpha \\ \alpha & \bar{\alpha} & \bar{\alpha} \\ \bar{\alpha} & \alpha & \bar{\alpha} \end{pmatrix}$, α = 0.3344(1)
V [Å^3]	1267.7(2)
d [g·cm^{-3}]	4.4437(2)
λ [Å]	0.73138
2*θ*-range [°], sin*θ*/*λ* (max)	34.92, 0.410
Index range	$0 \le h \le 10$ $-3 \le m_1 \le 3$ $-9 \le k \le 10$ $-3 \le m_2 \le 3$ $-8 \le l \le 10$ $-3 \le m_3 \le 3$
Independent reflections	1032
Parameters: profile/background/atoms	9/12/32
R_I, R_P, R_{WP} [%]	1.33, 3.76, 5.70
In1 at 8*a* ($^1/_8$ $^1/_8$ $^1/_8$) / U_{iso} [Å^2], SOF	0.0447(9), 0.650(1)
In2 at 16*d* ($^1/_4$ 0 $^3/_4$) / U_{iso} [Å^2]	0.0530(7), 0.961(1)
S at 32*e* (*u u u*) / U_{iso} [Å^2]	0.2572(1) / 0.0365(9)
4 × In1-S, [Å]	2.478(1)
6 × In2-S, [Å]	2.630(1)

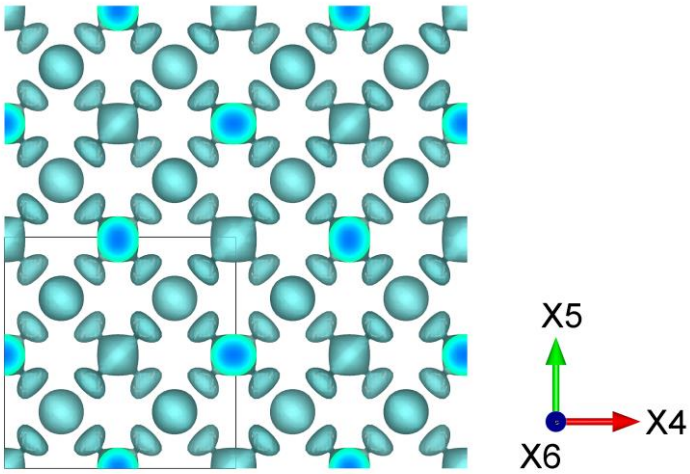

Figure S5. A distribution of 3D-function of the site occupancy factors (SOF) in the additional coordinates of the modulated structure (x_4, x_5, x_6) within (0–2, 0–2, 0–2)-ranges for In1-atoms at the isosurface with SOF = 0.65.

As one can see from Figure S5, the maxima of the statistical distribution of the positions' occupancies for In1-atoms depending on the additional coordinates of the modulated structure might reveal a partially incommensurate ordering of atoms.

Table S10. Modulation amplitudes of the displacive modulation in $In_{0.67}\square_{0.33}In_2S_4$ at 693 K.

Atom	$F^{(i)}_{xyz}$	U
In1	$F^{(1)}_{z}$	0.0018(3)
	$F^{(2)}_{xyz}$	-0.0005(1)
	$F^{(3)}_{z}$	0.0001(5)
	$F^{(4)}_{xyz}$	0.0007(1)
	$F^{(5)}_{z}$	-0.0007(2)
	$F^{(6)}_{xyz}$	0.0002(1)
In2	$F^{(7)}_{z}$	0.0024(2)
	$F^{(8)}_{xyz}$	0.0005(1)
	$F^{(9)}_{z}$	-0.0022(2)
	$F^{(10)}_{xyz}$	0.0010(1)
S	$F^{(11)}_{z}$	0.0120(2)
	$F^{(12)}_{xyz}$	-0.0025(2)
	$F^{(13)}_{xyz}$	0.0017(1)
	$F^{(14)}_{xyz}$	0.0053(1)
	$F^{(15)}_{z}$	0.0032(3)
	$F^{(16)}_{xyz}$	0.0026(2)
	$F^{(17)}_{xyz}$	0.0010(4)
	$F^{(18)}_{xyz}$	0.0009(2)

Table S11. Occupational modulation amplitudes in $In_{0.67}\square_{0.33}In_2S_4$ at 693 K.

Atom	F_p	U
In1	$F^{(19)}$	0.002(1)
	$F^{(20)}$	-0.003(2)
	$F^{(21)}$	0.005(2)
In2	$F^{(22)}$	-0.021(2)
	$F^{(23)}$	0.010(4)

$$p = p_0 + \sum_i U^i F^i(x_4, x_5, x_6)_p$$

Modulation functions for sine and cosine of Fourier terms:

$$x = x_0 + \sum_i U^i F^i(x_4,\ x_5, x_6)_x;\ y = y_0 + \sum_i U^i F^i(x_4,\ x_5, x_6)_y;\ z = z_0 + \sum_i U^i F^i(x_4,\ x_5, x_6)_z$$

$F^{(1)} = [\cos(2x_4+2x_5)-\cos(2x_4-2x_5)]_z$

$F^{(2)} = [\sin(2x_4+2x_5)+\sin(2x_4-2x_5)+\sin(2x_4+2x_6)+\sin(2x_4-2x_6)]_x +$
$+ [\sin(2x_4+2x_5)-\sin(2x_4-2x_5)+\sin(2x_5+2x_6)+\sin(2x_5-2x_6)]_y +$
$+ [\sin(2x_5+2x_6)-\sin(2x_5-2x_6)+\sin(2x_4+2x_6) -\sin(2x_4-2x_6)]_z;$

$F^{(3)} = [\cos(x_4+x_5+3x_6)+\cos(x_4+x_5-3x_6)-\cos(x_4-x_5-3x_6)-\cos(x_4-x_5+3x_6)]_z;$

$F^{(4)} = [\cos(x_4+3x_5+x_6)-\cos(x_4-3x_5+x_6)-\cos(x_4+3x_5-x_6)+\cos(x_4-3x_5-x_6) +$
$+ \cos(x_4+x_5+3x_6)-\cos(x_4+x_5-3x_6)+\cos(x_4-x_5-3x_6)-\cos(x_4-x_5+3x_6)]_x +$
$+ [\cos(3x_4+x_5+x_6)-\cos(3x_4-x_5-x_6)+\cos(3x_4-x_5+x_6)-\cos(3x_4+x_5-x_6) +$
$+ \cos(x_4+x_5+3x_6)-\cos(x_4+x_5-3x_6)-\cos(x_4-x_5-3x_6)+\cos(x_4-x_5+3x_6)]_y +$
$+ [\cos(3x_4+x_5+x_6)-\cos(3x_4-x_5-x_6)-\cos(3x_4-x_5+x_6)+\cos(3x_4+x_5-x_6) +$
$+ \cos(x_4+3x_5+x_6)-\cos(x_4-3x_5+x_6)+\cos(x_4+3x_5-x_6)-\cos(x_4-3x_5-x_6)]_z;$

$F^{(5)} = [\sin(3x_4+x_5+x_6)+\sin(3x_4-x_5-x_6)+\sin(3x_4-x_5+x_6)+\sin(3x_4+x_5-x_6)]_x +$
$+ [\sin(x_4+3x_5+x_6)-\sin(x_4-3x_5+x_6)+\sin(x_4+3x_5-x_6)-\sin(x_4-3x_5-x_6)]_y +$
$+ [\sin(x_4+x_5+3x_6)-\sin(x_4+x_5-3x_6)-\sin(x_4-x_5-3x_6)+\sin(x_4-x_5+3x_6)]_z;$

$F^{(6)} = [\sin(x_4+3x_5+x_6)+\sin(x_4-3x_5+x_6)+\sin(x_4+3x_5-x_6)+\sin(x_4-3x_5-x_6) +$
$+ \sin(x_4+x_5+3x_6)+\sin(x_4+x_5-3x_6)+\sin(x_4-x_5-3x_6)+\sin(x_4-x_5+3x_6)]_x +$
$+ [\sin(3x_4+x_5+x_6)-\sin(3x_4-x_5-x_6)-\sin(3x_4-x_5+x_6)+\sin(3x_4+x_5-x_6) +$
$+ \sin(x_4+x_5+3x_6)+\sin(x_4+x_5-3x_6)-\sin(x_4-x_5-3x_6)-\sin(x_4-x_5+3x_6)]_y +$
$+ [\sin(3x_4+x_5+x_6)-\sin(3x_4-x_5-x_6)+\sin(3x_4-x_5+x_6)-\sin(3x_4+x_5-x_6) +$
$+ \sin(x_4+3x_5+x_6)+\sin(x_4-3x_5+x_6)-\sin(x_4+3x_5-x_6)-\sin(x_4-3x_5-x_6)]_z;$

$F^{(7)} = [\sin(2x_5+2x_6)+\sin(2x_4+2x_6)]_z;$

$F^{(8)} = [\sin(2x_5+2x_6)]_x+[\sin(2x_4+2x_6)]_y+[\sin(2x_4+2x_5)]_z;$

$F^{(9)} = [\sin(3x_4+x_5+x_6)+\sin(x_4+3x_5+x_6)+\sin(x_4+x_5+3x_6)]_z;$

$F^{(10)}= [\sin(x_4+3x_5+x_6)+\sin(x_4+x_5+3x_6)]_x+[\sin(3x_4+x_5+x_6)+\sin(x_4+x_5+3x_6)]_y +$
$+ [\sin(3x_4+x_5+x_6)+\sin(x_4+3x_5+x_6)]_z;$

$F^{(11)} = [\cos(2x_5+2x_6)+\cos(2x_4+2x_6)]_z;$

$F^{(12)} = [\cos(2x_5+2x_6)]_x+[\cos(2x_4+2x_6)]_y+[\cos(2x_4+2x_5)]_z;$

$F^{(13)} = [\sin(2x_4+2x_5)+\sin(2x_4+2x_6)]_x+[\sin(2x_4+2x_5)+\sin(2x_5+2x_6)]_y +$
$+ [\sin(2x_5+2x_6)+\sin(2x_4+2x_6)]_z;$

$F^{(14)} = [\sin(2x_5+2x_6)]_x+[\sin(2x_4+2x_6)]_y+[\sin(2x_4+2x_5)]_z;$

$F^{(15)} = [\cos(3x_4+x_5+x_6)+\cos(x_4+3x_5+x_6)+\cos(x_4+x_5+3x_6)]_z;$

$F^{(16)} = [\cos(x_4+3x_5+x_6)+\cos(x_4+x_5+3x_6)]_x+[\cos(3x_4+x_5+x_6)+\cos(x_4+x_5+3x_6)]_y +$
$+ [\cos(3x_4+x_5+x_6)+\cos(x_4+3x_5+x_6)]_z;$

$F^{(17)} = [\sin(3x_4+x_5+x_6)]_x+[\sin(x_4+3x_5+x_6)]_y+[\sin(x_4+x_5+3x_6)]_z;$

$F^{(18)} = [\sin(x_4+3x_5+x_6)+\sin(x_4+x_5+3x_6)]_x+[\sin(3x_4+x_5+x_6)+\sin(x_4+x_5+3x_6)]_y +$
$+ [\sin(3x_4+x_5+x_6)+\sin(x_4+3x_5+x_6)]_z;$

$F^{(19)} = [\cos(2x_4+2x_5)+\cos(2x_4-2x_5)+\cos(2x5+2x6) +$
$+ \cos(2x_5-2x_6)+\cos(2x_4+2x_6)+\cos(2x4-2x6)]_p;$

$F^{(20)} = [\cos(3x_4+x_5+x_6)+\cos(3x_4-x_5-x_6)+\cos(3x_4-x_5+x_6) +$
$+ \cos(3x_4+x_5-x_6)+\cos(x_4+3x_5+x_6)+\cos(x_4-3x_5+x_6) +$
$+ \cos(x_4+3x_5-x_6)+\cos(x_4-3x_5-x_6)+\cos(x_4+x_5+3x_6) +$
$+ \cos(x_4+x_5-3x_6)+\cos(x_4-x_5-3x_6)+\cos(x_4-x_5+3x_6)]_p;$

$F^{(21)} = [\sin(3x_4+x_5+x_6)+\sin(3x_4-x_5-x_6)-\sin(3x_4-x_5+x_6) -$
$+ \sin(3x_4+x_5-x_6)+\sin(x_4+3x_5+x_6)-\sin(x_4-3x_5+x_6) -$
$+ \sin(x_4+3x_5-x_6)+\sin(x_4-3x_5-x_6)+\sin(x_4+x_5+3x_6) -$
$+ \sin(x_4+x_5-3x_6)+\sin(x_4-x_5-3x_6)-\sin(x_4-x_5+3x_6)]_p;$

$F^{(22)} = [\cos(2x_4+2x_5)+\cos(2x_5+2x_6)+\cos(2x_4+2x_6)]_p;$

$F^{(23)} = [\cos(3x_4+x_5+x_6)+\cos(x_4+3x_5+x_6)+\cos(x_4+x_5+3x_6)]_p;$

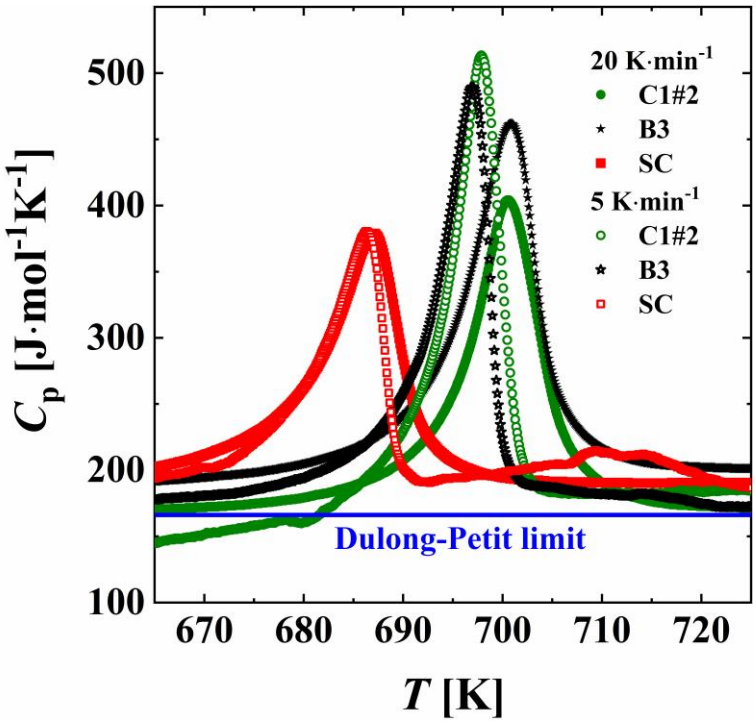

Figure S6. Molar heat capacity of C1#2-, B3- and SC1-samples in the vicinity of the α-β phase transition range measured with heating rates of 5 and 20 K·min^{-1}. Polycrystalline samples reveal endothermic peak within narrow onset temperature 688 K < T_{onset} < 694 K. The lower T_{onset} for single-crystalline sample (T_{onset} = 674 K) might be attributed to the presence of twin domains.

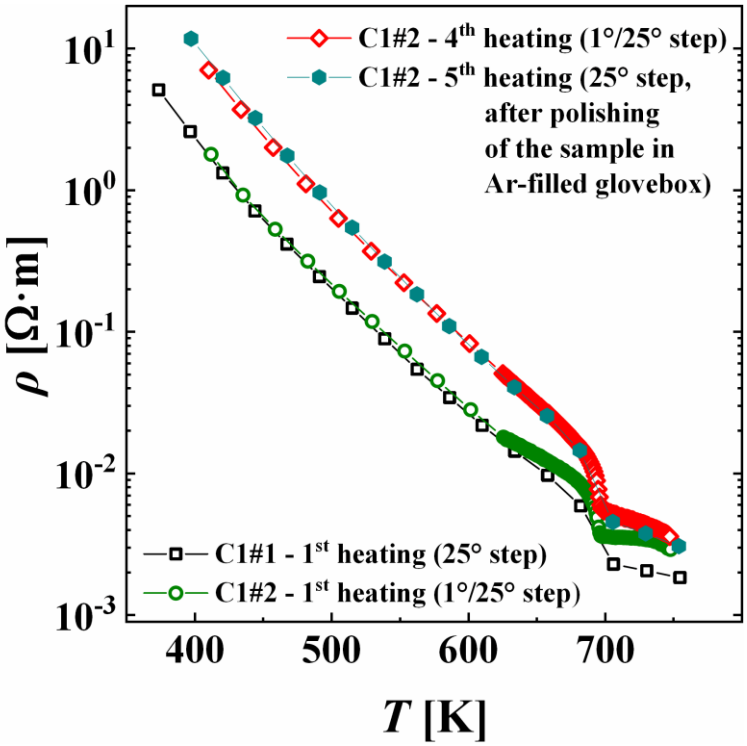

Figure S7. Electrical resistivity for samples C1#1 and C1#2, obtained in parallel SPS-processes. Below the phase transition, values agree well for both specimens, proving a reproducibility of the SPS-procedure and a good homogeneity of the obtained pellets. Further cycles lead to an increase of resistivity, independent from in-between-polishing of the sample (performed in an argon-filled glovebox).